Electronic Supplementary Material (ESI) for Journal of Materials Chemistry A.

Supporting Information

Hierarchical mesoporous $NiFe_2O_4$ nanocone forest directly growing on carbon textile for high performance flexible supercapacitors

Muhammad Sufyan Javed[1,2], Cuilin Zhang[1], Lin Chen[1], Yi Xi[1], Chenguo Hu[1]*

[1]*Department of Applied Physics, Chongqing University, Chongqing 400044, P. R. China*

[2]*Department of Physics, COMSATS Institute of Information Technology Lahore 54000, Pakistan*

**Corresponding author. Tel: +86 23 65670880; Fax: +86 23 65678362*

E-mail address hucg@cqu.edu.cn (CG Hu)

1. **Figure S1**. Optical photographs of carbon textile and supercapacitors. (A) Pristine carbon textile, (B) NFO assembled carbon textile after annealing at 350 ^{o}C for 2h, (C) As-prepared single electrode and (D) As-fabricated solid state supercapacitors.
2. **Figure S2.** SEM images of NFO precursor and after annealing process at different magnifications. (A) NFO nanocone forest precursor, (B) SEM image of NFO after heat treatment, (C) Selected part from Figure B, (D) high resolution SEM of image of NFO nanocone forest.
3. **Figure S3.** (A) N_2 adsorption–desorption isotherm, (B) BJH adsorption pore size distribution of $NiFe_2O_4$ nanocone forest.
4. **Figure S4.** Electrochemical performances of the $NiFe_2O_4$ nanoforest single electrode in 6 M of LiCl aqueous electrolyte. (A) CV curves at different scan rates ranging from 5 to 100 m Vs^{-1} in potential window of -0.2 to 0.7 V, (B) Specific capacitance as a function scan rate.
5. **Figure S5.** XRD pattern of the electrode before and after 50 cycles at charging state at room temperature. The peaks for the electrode after 50 cycles are in agreement with standard values of Carbon textile (CT), Li_2O, Ni and Fe from JCPDS cards (Graphite: 752078; Li_2O: 772144; Ni: 882326; Fe: 870722).
6. **Figure S6.** Electrochemical performances of the $NiFe_2O_4$ nanoforest single electrode in 6 M of LiCl aqueous electrolyte. (A) Charging-discharging curves taken at different current densities ranging from 1 to 6 A/g in potential window of 0 to 0.45 V, (B) Nyquist plot of impedance from 0.01 to 100 kHz at open circuit potential.
7. **Figure S7.** The comparison of CV curves of bare CT based supercapacitor and $NiFe_2O_4$ assembled CT based supercapacitor at scan rate of 50 mV s^{-1}.
8. **Figure S8.** (A) Low resolution SEM image of the $NiFe_2O_4$ nanocone forest after 10,000 cycles (inset arrow shows the layer of gel electrolyte), (B) high resolution SEM image.

9. **Calculation details**

1. Figure S1.

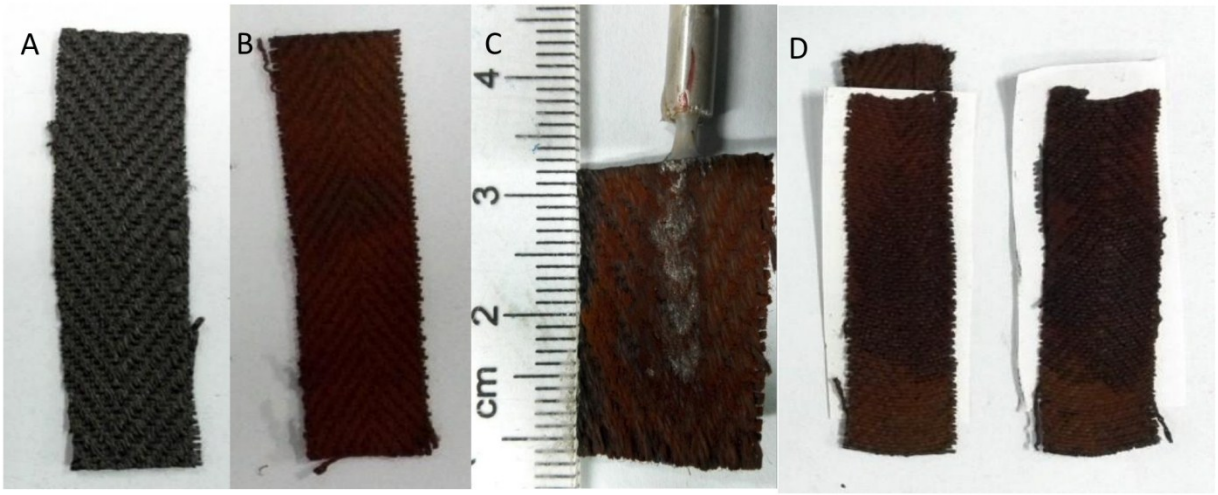

Figure S1. Optical photographs of carbon textile and supercapacitors. (A) Pristine carbon textile, (B) $NiFe_2O_4$ assembled carbon textile after annealing at 350 ^oC for 2h, (C) As-prepared single electrode, (D) Optical photographs of as-fabricated solid state supercapacitors.

2. Figure S2

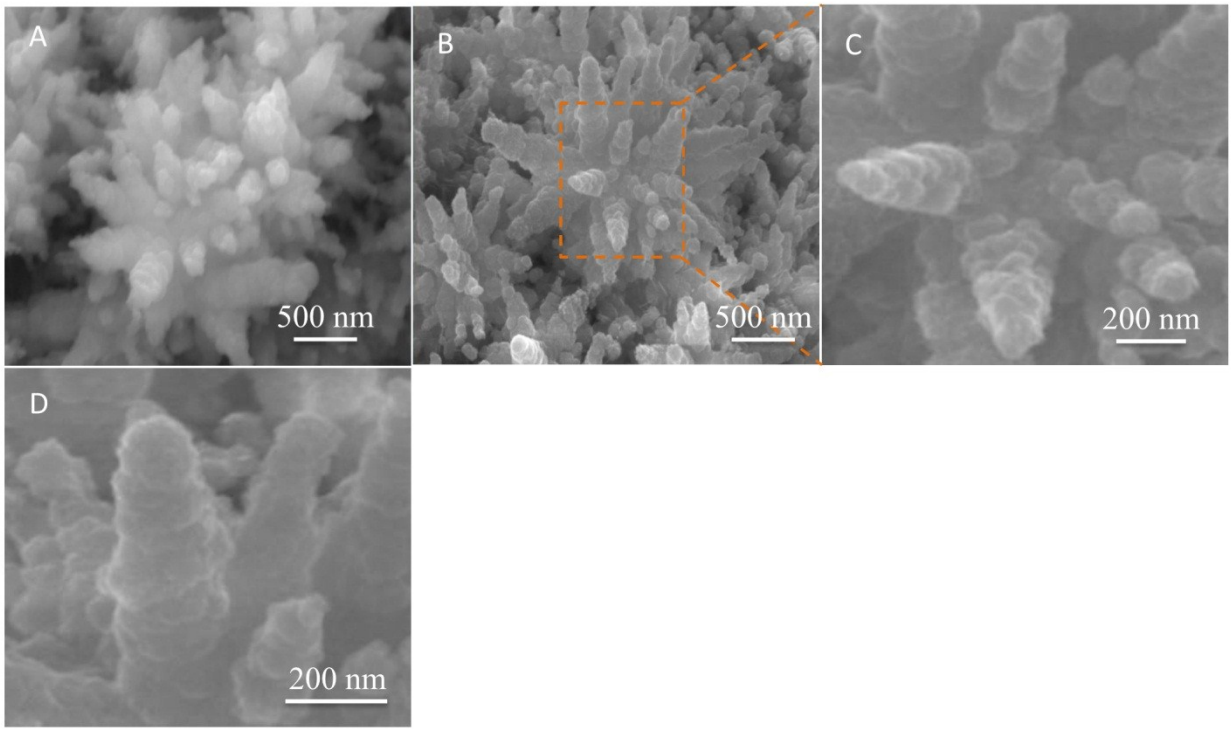

Figure S2. SEM images of NFO precursor and after annealing process at different magnifications. (A) NFO nanocone forest precursor, (B) SEM image of NFO after heat treatment, (C) Selected part from Figure B, (D) high resolution SEM of image of NFO nanocone forest.

3. Figure S3

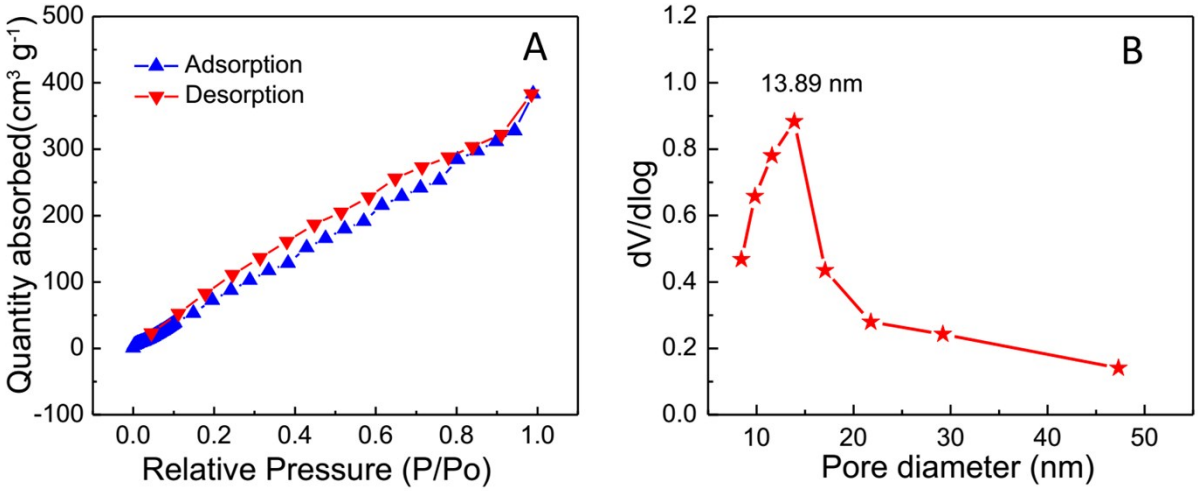

Figure S3: (A) N2 adsorption–desorption isotherm, (B) BJH adsorption pore size distribution of $NiFe_2O_4$ nanocone forest.

4. Figure S4

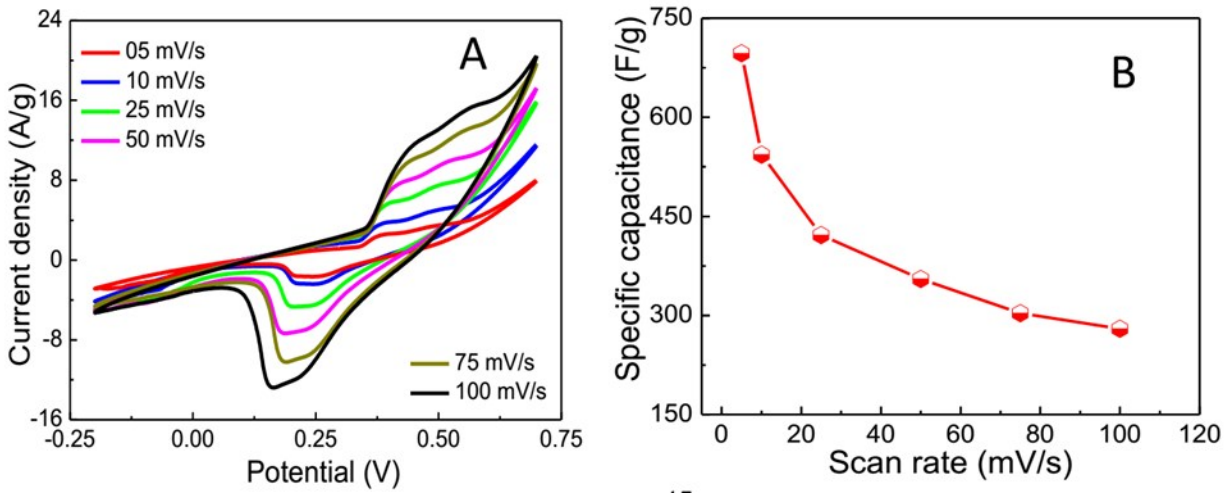

Figure S4. Electrochemical performances of the $NiFe_2O_4$ nanoforest single electrode in 6 M of LiCl aqueous electrolyte. (A) CV curves at different scan rates ranging from 5 to 100 m Vs^{-1} in potential window of -0.2 to 0.7 V, (B) Specific capacitance as a function scan rate.

5. Figure S5.

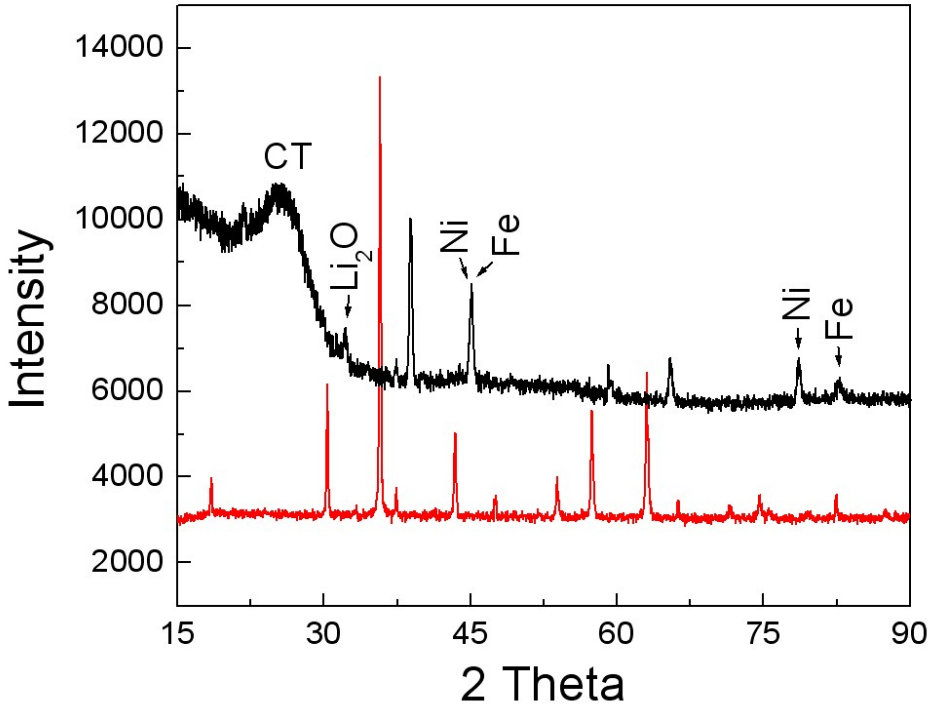

Figure S5. XRD pattern of the electrode before and after 50 cycles at charging state at room temperature. The peaks for the electrode after 50 cycles are in agreement with standard values of Carbon textile (CT), Li_2O, Ni and Fe from JCPDS cards (Graphite: 752078; Li_2O: 772144; Ni: 882326; Fe: 870722). In the same time, we also found the shift of the peaks of $NiFe_2O_4$, which means the deformation of the crystal structure of the $NiFe_2O_4$. The further investigation will be also very interesting and we are planning to carry out in the recent future.

6. Figure S6.

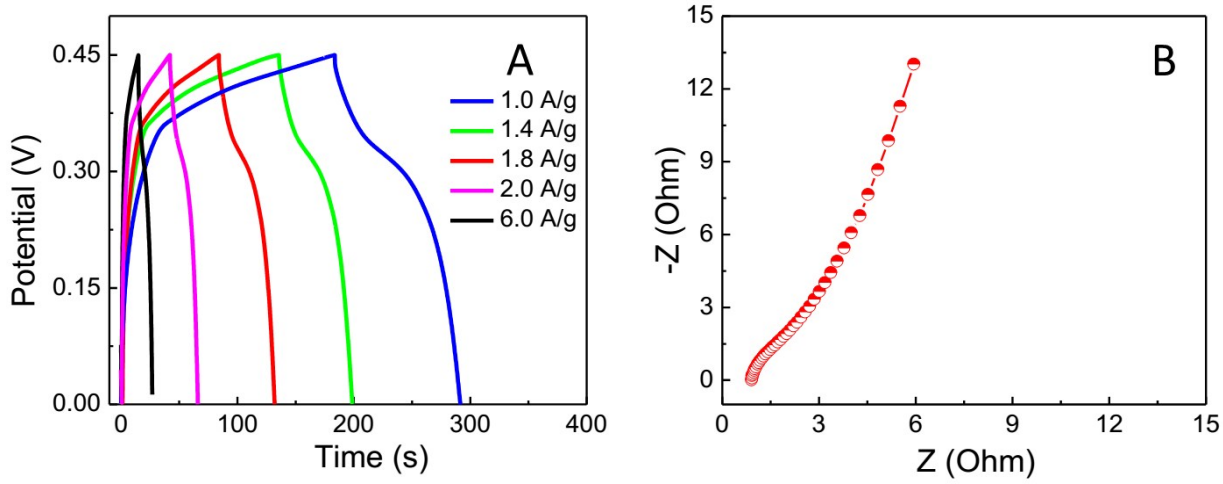

Figure S6. Electrochemical performances of the $NiFe_2O_4$ nanoforest single electrode in 6 M of LiCl aqueous electrolyte. (A) Charging-discharging curves taken at different current densities ranging from 1 to 6 A/g in potential window of 0 to 0.45 V, (B) Nyquist plot of impedance from 0.01 to 100 kHz at open circuit potential.

7. Figure S7.

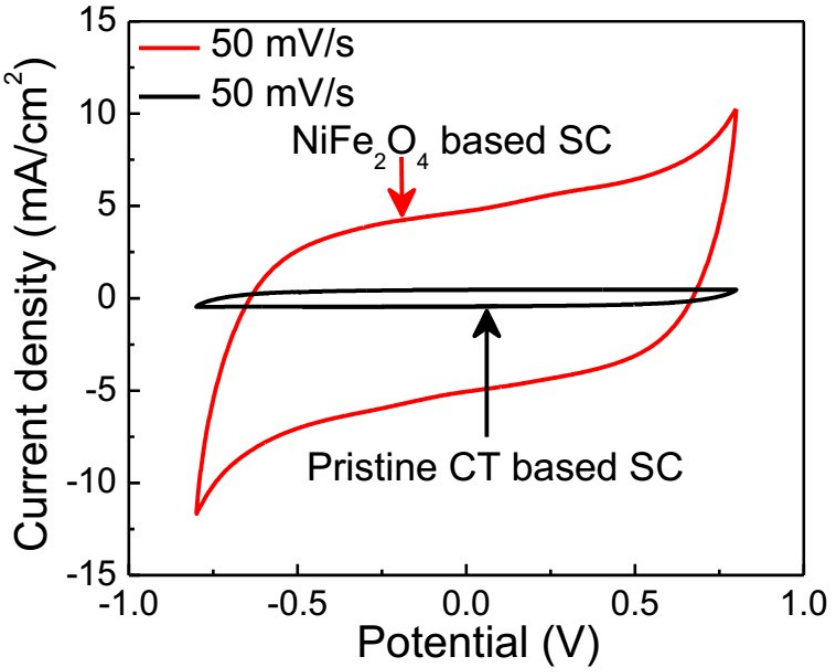

Figure S7: The comparison of CV curves of bare CT based supercapacitor and $NiFe_2O_4$ assembled CT based supercapacitor at scan rate of 50 mV s^{-1}.

8. Figure S8

Figure S8. (A) Low resolution SEM image of the $NiFe_2O_4$ nanocone forest after 10,000 cycles (the arrow shows the layer of gel electrolyte), (B) high resolution SEM image.

9. Calculation details

The specific capacitance (C_{sp}), energy density (ED) and power density (PD) of single electrode and solid state supercapacitor were calculated according to the following equations.[1-4]

$$C_{sp} = \frac{\int I(A)\,dV}{M\,v\,(V_f - V_i)} \quad (1)$$

$$E = CV^2 \times \left(\frac{5}{36}\right) \quad (2)$$

$$P = \frac{E}{t_d} = \frac{I\Delta V}{2M} \times 1000 \quad (3)$$

Where C_{sp} (F g^{-1}) is the specific capacitance; $\int I(A)\,dV$ is the area of CV curve; A is the active area of supercapacitor; M (g) is the mass of active material on one electrode; $\Delta V = V_f - V_i$ is the potential window; v (Vs^{-1}) is the scan rate; I (A) is the applied current; P (W kg^{-1}) is the power density; E (Wh kg^{-1}) is the energy density; t_d is charging time (s), respectively.

1. M. S. Javed, S. Dai, M. Wang, Y. Xi, Q. Leng, D. Guo and C. Hu, *Nanoscale*, 2015.
2. K. Zhang, H. Chen, X. Wang, D. Guo, C. Hu, S. Wang, J. Sun and Q. Leng, *Journal of Power Sources*, 2014, 268, 522-532.
3. M. S. Javed, S. Dai, M. Wang, D. Guo, L. Chen, X. Wang, C. Hu and Y. Xi, *J. Power Sources*, 2015, 285, 63-69.
4. M. S. Javed, J. Chen, L. Chen, Y. Xi, C. Zhang, B. Wan and C. Hu, *J. Mater. Chem. A*, 2016, 4, 667-674.